Superconducting and magnetic properties of $Sr_3Ir_4Sn_{13}$

P. K. Biswas,[1,*] A. Amato,[1] R. Khasanov,[1] H. Luetkens,[1] Kefeng Wang,[2] C. Petrovic,[2] R. M. Cook,[3] M. R. Lees,[3] and E. Morenzoni[1,†]

[1]*Laboratory for Muon Spin Spectroscopy, Paul Scherrer Institute, CH-5232 Villigen PSI, Switzerland*

[2]*Condensed Matter Physics and Materials Science Department, Brookhaven National Laboratory, Upton, New York 11973, USA*

[3]*Physics Department, University of Warwick, Coventry, CV4 7AL, United Kingdom*

(Received 24 March 2014; revised manuscript received 24 September 2014; published 10 October 2014)

Magnetization and muon spin rotation and relaxation (μSR) measurements have been performed to study the superconducting and magnetic properties of $Sr_3Ir_4Sn_{13}$. From magnetization measurements the lower and upper critical fields $T = 0$ K are found to be 8.5(1) mT and 1.44(2) T, respectively. Zero-field μSR data show no sign of any magnetic ordering or weak magnetism. Transverse-field μSR measurements in the vortex state provide the temperature dependence of the magnetic penetration depth λ. The temperature dependence of λ^{-2} is consistent with the existence of a single s-wave energy gap in the superconducting state of $Sr_3Ir_4Sn_{13}$ with a gap value of 0.82(2) meV at absolute zero temperature. However, a two-gap $s + s$-wave model fit with gap values of 0.91(4) and 0.14(7) meV cannot be ruled out completely. The magnetic penetration depth at zero temperature $\lambda(0)$ is 291(3) nm. The ratio $\Delta(0)/k_BT_c = 2.1(1)$ indicates that $Sr_3Ir_4Sn_{13}$ should be considered a strong-coupling superconductor.

DOI: 10.1103/PhysRevB.90.144505 PACS number(s): 74.25.Ha, 74.70.Dd, 76.75.+i

Recently, ternary intermetallic stannide compounds, $R_3Ir_4Sn_{13}$ where $R =$ Ca, Sr, etc., have attracted renewed interest because of the possible coexistence of superconducting and charge density wave states and the presence of pressure induced structural quantum phase transitions [1]. $Sr_3Ir_4Sn_{13}$ superconducts below the transition temperature $T_c \simeq 5$ K, whereas the sister compound, $Ca_3Ir_4Sn_{13}$, becomes superconducting below $\simeq$7 K [2]. Since the size of a Ca ion is smaller than that of a Sr ion, the substitution of Ca on the Sr site corresponds to applying positive pressure, which then enhances the T_c in the Ca compound. This trend continues in $Ca_3Ir_4Sn_{13}$ with the application of external pressure. Under hydrostatic pressure, the T_c of $Ca_3Ir_4Sn_{13}$ increases to 8.9 K at 4 GPa and then falls for higher pressures [1]. An increase of T_c with increasing pressure has also been observed for $Sr_3Ir_4Sn_{13}$, a behavior at variance with that of a conventional phonon-mediated BCS superconductor. In $Sr_3Ir_4Sn_{13}$, an anomaly at $T^* \simeq 147$ K has been detected in resistivity and susceptibility measurements. The equivalent anomaly occurs at $T^* \simeq 33$ K in the $Ca_3Ir_4Sn_{13}$ and was initially attributed to ferromagnetic (FM) spin fluctuations, coexisting with the superconductivity appearing at lower temperature [3]. Later, single crystal x-ray diffraction studies [1] showed that the T^* anomaly in $Sr_3Ir_4Sn_{13}$ is produced by a second-order superlattice transition from a simple cubic parent phase, the I phase, to a superlattice structure, the I' phase, with a lattice parameter twice that of the I phase. It has been further argued that this superlattice transition is associated with a charge density wave (CDW) transition of the conduction electron system. Both the Hall and Seebeck coefficients indicate that at T^* a gap opens and that there is significant Fermi surface reconstruction at T^* in $Ca_3Ir_4Sn_{13}$ [4]. Whereas a low $\frac{T_c}{T_F}$ (T_F is the Fermi temperature) ratio from thermoelectricity data points to a weakly correlated superconductor [4], other parameters such as the Wilson and Kadowaki-Woods ratios close to those of heavy fermions have been taken as indicative of a more strongly correlated system [3]. Specific heat measurements on $R_3T_4Sn_{13}$ ($R =$ Sr, La, $T =$ Ir, Rh) and $Ca_3Ir_4Sn_{13}$ [3,5] suggest nodeless superconductivity and strong coupling, but thermal conductivity data on $Ca_3Ir_4Sn_{13}$ did not exclude either a single anisotropic gap, or the presence of multiple isotropic gaps with different magnitudes [6]. A recent μSR study on $Ca_3Ir_4Sn_{13}$ [7] determined a very high gap-to-T_c ratio value $\Delta(0)/(k_BT_c) \approx 5$, which is unusually large even for a very strongly coupled BCS superconductor and much larger than the value of 2.53 inferred from macroscopic measurements [8]. In order to obtain a better insight into the nature of the superconducting and magnetic state of these intermetallic stannide compounds and try to understand the sources of the differences between the experimental results obtained for these compounds, we have performed μSR and magnetization measurements on $Sr_3Ir_4Sn_{13}$, which is isoelectronic to $Ca_3Ir_4Sn_{13}$.

Single crystal samples of $Sr_3Ir_4Sn_{13}$ were grown and characterized as described in Ref. [4]. Magnetization measurements were performed using an Oxford Instruments vibrating sample magnetometer (VSM). For all the magnetization measurements, the data were corrected for demagnetization effects using the method described in Ref. [9]. The sample was a rod-shaped single crystal with dimensions $(2.1 \times 0.8 \times 0.4)$ mm^3 and the magnetic field was applied parallel to the long axis of the sample. The demagnetization factor D of the sample was approximately 0.1 in SI units. The transverse-field (TF)- and zero-field (ZF)-μSR experiments were carried out using the Dolly instrument (πE1 beam line) and at the new high field and low temperature instrument (HAL-9500, πE3 beam line) of the Paul Scherrer Institute (Villigen, Switzerland). The sample was cooled to the base temperature in zero field for the ZF-μSR experiments and in 50 mT for the TF-μSR experiments. Typically, $\sim$10 million muon decay events were collected for each spectrum. However, in the normal state only half of these counts were collected, because the muon spin

*pabitra.biswas@psi.ch

†elvezio.morenzoni@psi.ch

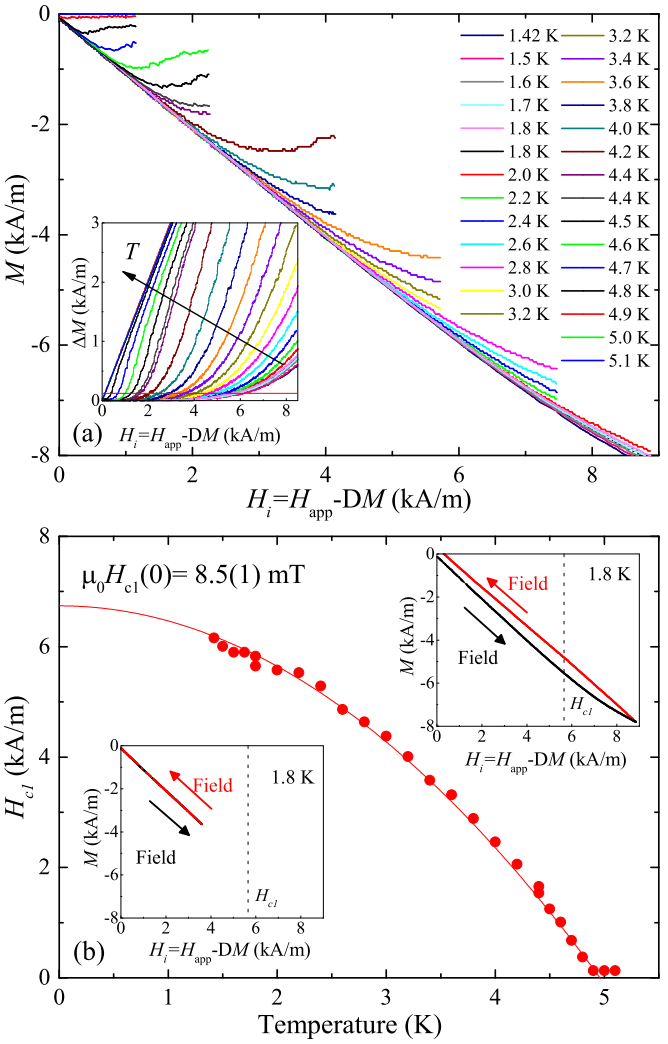

FIG. 1. (Color online) (a) Low-field virgin magnetization curves of $Sr_3Ir_4Sn_{13}$, collected at different temperatures. The inset shows the departure from linearity ΔM, calculated by subtracting the linear fit from each of the M vs H curves. (b) Temperature dependence of H_{c1}. The solid line is a quadratic fit to the data using Eq. (1). The insets show the M vs H curves up to two different maximum applied field values (above and below the H_{c1} value at 1.8 K) that validate our estimate of H_{c1}.

depolarization above T_c is weak and temperature independent. The ZF- and TF-μSR data were analyzed by using the free software package MUSRFIT [10].

Figure 1(a) shows the virgin magnetization M versus applied field H_i collected at various temperatures. These measurements were performed to obtain the temperature dependence of the lower critical field H_{c1} by estimating the deviation from linearity in each of the M vs H_i curves. To do this, a linear fit to data was made for very low applied fields. The departure from linearity ΔM was calculated by subtracting the linear fit from each of the M vs H_i curves [see the inset of Fig. 1(a)] and the field H_{c1} at each temperature was determined by using the criterion $\Delta M = 125$ A/m, indicated in the inset as a solid horizontal line. This method is generally accepted as a reasonable way to estimate H_{c1} and was used, for instance, in studies of high-T_c cuprate materials [11]. Figure 1(b) shows $H_{c1}(T)$ for $Sr_3Ir_4Sn_{13}$. The solid line, which is a quadratic fit to the data, using

$$H_{c1}(T) = H_{c1}(0)\left\{1 - \left(\frac{T}{T_c}\right)^2\right\}, \quad (1)$$

appears to give a fair estimate for $H_{c1}(0)$. We obtain $H_{c1}(0) = 6.74(5)$ kA/m ($\mu_0 H_{c1}(0) = 8.5(1)$ mT). The error given is purely statistical. We estimate the systematic error to be about 10%. We then checked our estimate of $H_{c1}(T)$ by using the following procedure. In a first experiment, we zero-field cooled the sample from above T_c to 1.8 K and then increased the applied field up to 9 kA/m [well above $H_{c1}(1.8\,\text{K}) = 5.8$ kA/m, estimated from the fitted curve] and then decreased the field back to zero. The presence of hysteresis in the data [see the top inset of Fig. 1(b)] implies that in this case some flux lines have entered the sample and that the sample has crossed the H_{c1} limit to the mixed state. In a second experiment, we cooled the sample from above T_c to 1.8 K in zero field and then increased the applied field up to 4 kA/m [below $H_{c1}(1.8\,\text{K}) = 5.8$ kA/m]. In this case, the curve is completely reversible [see the bottom inset of Fig. 1(b)] confirming that the applied field remains well below the H_{c1} value at 1.8 K.

Figure 2(a) shows the first two quadrants of the M vs H loops collected at different temperatures to determine H_{c2}. Figure 2(b) shows a magnification of the red dotted area in Fig. 2(a). A secondary peak or fish tail effect is detected in the magnetization loop at an applied field close to H_{c2}. The peak effect slowly disappears as we move to higher temperatures. Similar peak effects have also been observed in many other weak pinning superconductors (see Ref. [12] and references therein). The presence of such a peak effect in $Sr_3Ir_4Sn_{13}$ may be an indication of additional pinning due to disorder. The temperature dependence of the upper critical field H_{c2} of $Sr_3Ir_4Sn_{13}$, determined from the point in the $M(H)$ loops where $\Delta M = 0$, is shown in Fig. 2(c). $H_{c2}(T)$ can be fit using the Werthamer-Helfand-Hohenberg (WHH) expression [13,14]. The model has two important parameters, α and λ_{so}. α is the Maki parameter and represents the strength of the Pauli paramagnetic effect, whereas λ_{so} is a measure of the strength of the spin-orbit scattering. In the fit, α was calculated to 0.22 using the expression, $\alpha = 0.528(-dH_{c2}/dT)|_{T=T_c}$ (T/K) [13]. The WHH fit yields $H_{c2}(0) = 1150(20)$ kA/m [$\mu_0 H_{c2}(0) = 1.44(2)$ T] and $\lambda_{so} = 1.406(2)$. A simple linear extrapolation of the data to $T = 0$ K gives $H_{c2} = 1430(10)$ kA/m [$\mu_0 H_{c2}(0) = 1.80(1)$ T] [15].

Figure 3(a) compares the ZF-μSR signals collected above and below T_c and above T^* at 150 K. The signals at 1.5 and 6.0 K are practically identical, implying that no additional magnetic moments (either static or dynamic) appear below T_c. However, the ZF-μSR signal taken at 150 K shows a lower relaxation rate than the ones at low temperatures. The ZF-μSR data can be well described using a Gaussian Kubo-Toyabe relaxation function [16],

$$A(t) = A(0)\left\{\frac{1}{3} + \frac{2}{3}(1 - \Lambda^2 t^2)\exp\left(-\frac{\Lambda^2 t^2}{2}\right)\right\}, \quad (2)$$

where $A(0)$ is the initial asymmetry and Λ describes the muon spin relaxation rate due to the presence of static nuclear

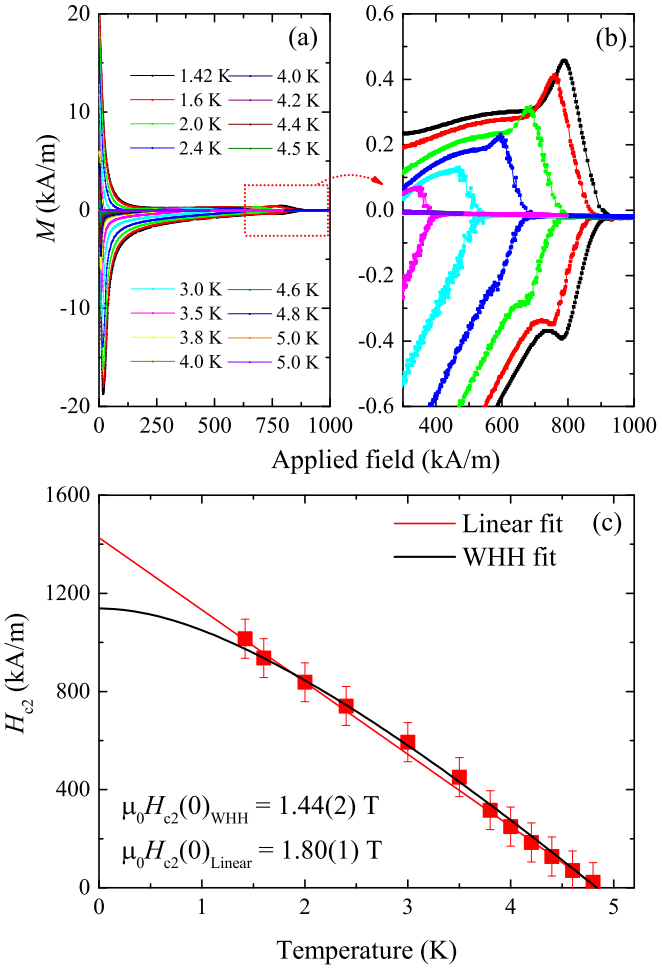

FIG. 2. (Color online) (a) M vs H loops, collected at different temperatures. (b) Magnified view of the data within the red dotted box in Fig. 2(a). (c) Temperature dependence of H_{c2} of $Sr_3Ir_4Sn_{13}$.

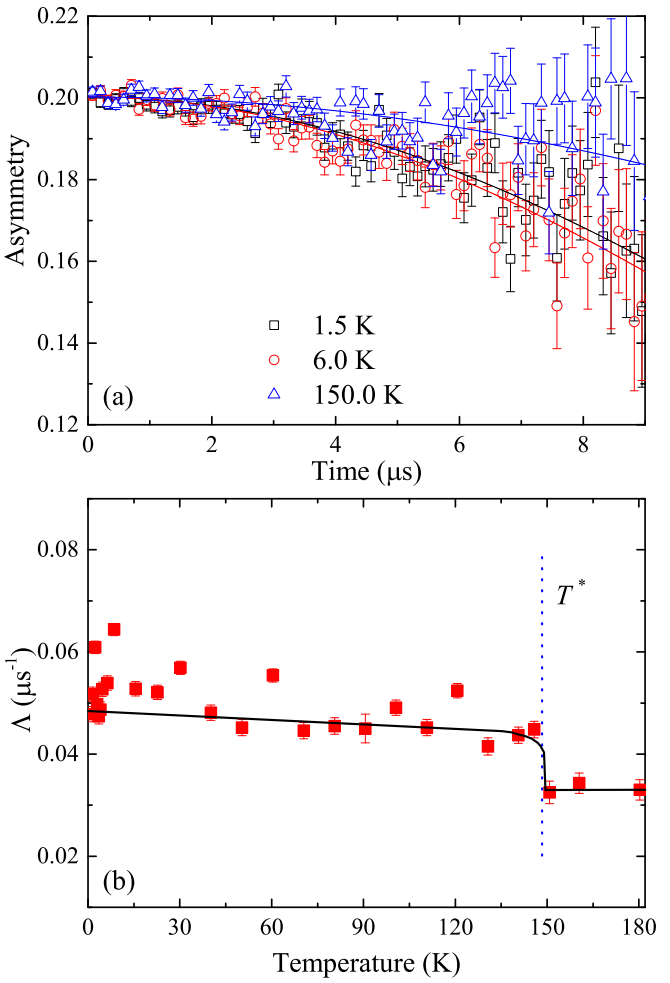

FIG. 3. (Color online) (a) ZF-μSR spectra of $Sr_3Ir_4Sn_{13}$ taken above (150 and 6 K) and below T_c (at 1.5 K). The solid lines are fits to the data using Eq. (2). (b) Temperature dependence of the muon spin relaxation rate in $Sr_3Ir_4Sn_{13}$ due to the presence of static nuclear moments. The solid line is a guide to the eye.

moments in $Sr_3Ir_4Sn_{13}$. The temperature dependence of Λ is shown in Fig. 3(b). A small and abrupt reduction of the relaxation rate is observed at ~150 K. Such a behavior is consistent with a structural phase transition or the onset of a CDW transition accompanied by strain or a lattice distortion at $T^* \simeq 147$ K. It may arise from concomitant changes in the muon position relative to the relevant nuclear moments and hence in the field distribution probed by a very sensitive local technique such as μSR. A change of Λ by ~30% corresponds to a change of the muon position with respect to the nuclear moments of ~10%. This is possible, given that the transition leads a doubling of the lattice constant and induces a distortion of the Sn icosahedrons with tilting of the IrSn trigonal prims connecting them [1]. In the sister compound $Ca_3Ir_4Sn_{13}$ no change of the ZF relaxation rate at $T^* \simeq 33$ K has been observed [7]. A possible explanation is that the nuclear moment density in Ca is about 70 times smaller than in Sr. Instead, a sudden drop in Λ at ~80 K has been attributed to muon diffusion. This appears very unlikely given the low temperature. Moreover, diffusion does not lead to sharp changes in relaxation rate as observed but generally displays Arrhenius-type behavior.

Figure 4 shows the TF-μSR precession signals of $Sr_3Ir_4Sn_{13}$ taken above (7.5 K) and below (18 mK) T_c in an applied field of 50 mT. The signal in the normal state shows almost no damping, reflecting the homogeneous magnetic field distribution in the bulk of the material, whereas it decays very quickly below T_c due to the inhomogeneous field distribution $p(B)$ generated by the vortex lattice [17].

From the TF-μSR spectra we can determine the second moment of the magnetic field distribution and from this the magnetic penetration depth. Since $p(B)$ can be well represented by a multicomponent Gaussian curve, the muon time spectra are fitted to a sum of N Gaussian components [18,19]:

$$A(t) = \sum_{i=1}^{N} A_i \exp\left(-\sigma_i^2 t^2/2\right)\cos(\gamma_\mu B_i t + \phi) + A_{bg}\cos(\gamma_\mu B_{bg} t + \phi), \quad (3)$$

where ϕ, A_i, σ_i, and B_i are the initial phase, asymmetry, relaxation rate, and mean field (first moment) of the ith Gaussian component, respectively. A_{bg} and B_{bg} are the asymmetry

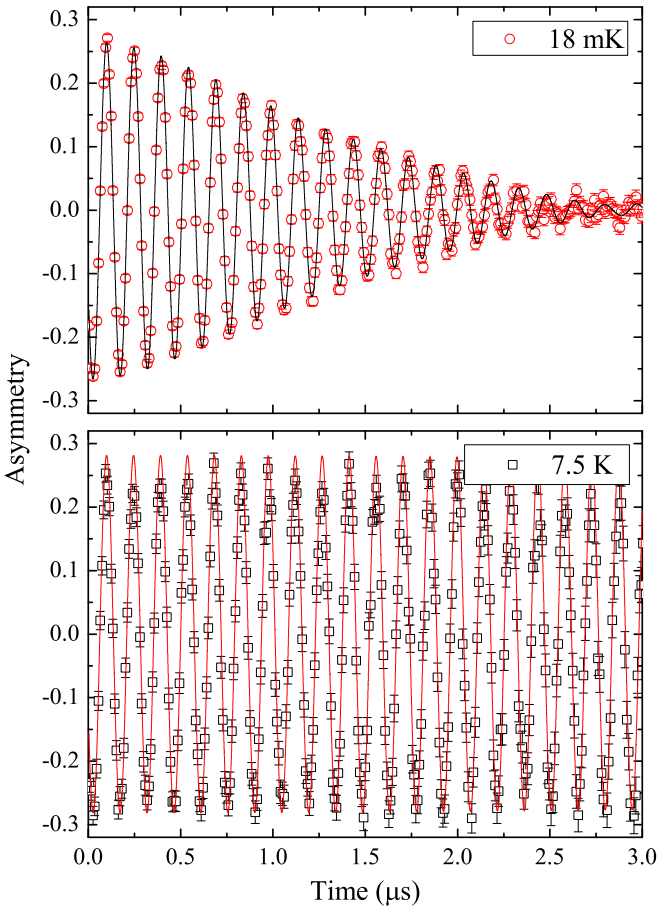

FIG. 4. (Color online) TF-μSR precession signals for $Sr_3Ir_4Sn_{13}$ measured above (at 7.5 K) and below (at 18 mK) T_c in an applied field of 50 mT. The solid lines are fits to the data using Eq. (3).

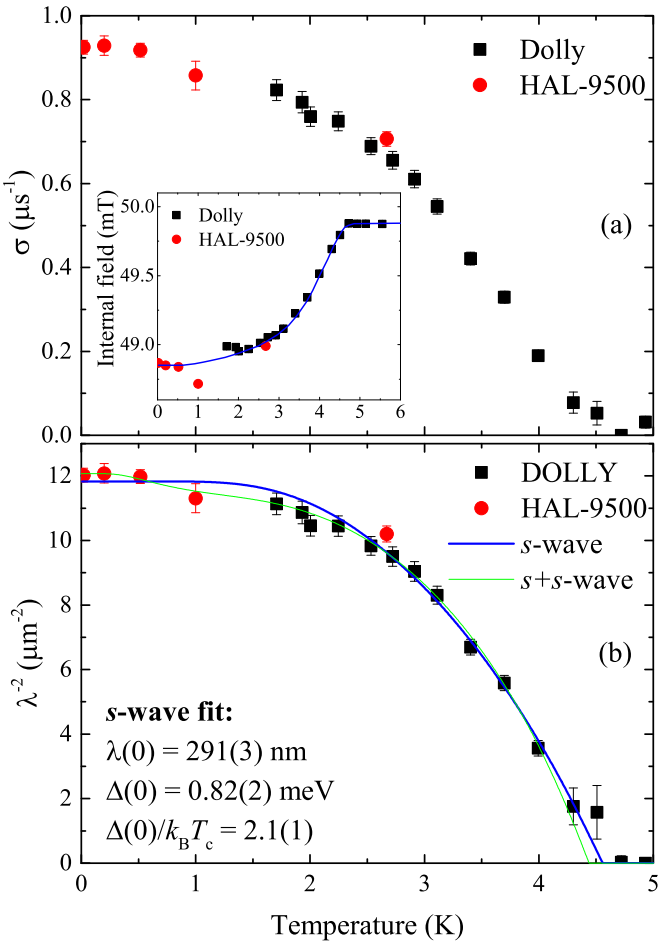

FIG. 5. (Color online) (a) Temperature dependence of the muon depolarization rate σ of $Sr_3Ir_4Sn_{13}$ collected on two spectrometers DOLLY and HAL-9500 at an applied magnetic field of 50 mT. The inset shows the typical diamagnetic shift of the internal field experienced by the muons below T_c. (b) Temperature dependence of $\lambda^{-2}(T)$. The solid lines are fits to the data using a single-gap s-wave model and a two-gap $s+s$-wave model.

and field, respectively, due to background contribution, mainly originating from the muons that miss the sample and hit the sample holder or the walls of the cryostat. We found that two Gaussian components ($N = 2$) are sufficient to fit the time spectra. For $N = 2$, the first and second moments of $p(B)$ are given by

$$\langle B\rangle = \sum_{i=1}^{2} \frac{A_i B_i}{A_1 + A_2}, \tag{4}$$

and

$$\langle \Delta B^2\rangle = \frac{\sigma^2}{\gamma_\mu^2} = \sum_{i=1}^{2} \frac{A_i}{A_1 + A_2}\{(\sigma_i/\gamma_\mu)^2 + [B_i - \langle B\rangle]^2\}, \tag{5}$$

where $\gamma_\mu/2\pi = 135.54$ MHz/T is the muon gyromagnetic ratio and σ the muon depolarization rate. Figure 5(a) shows the temperature dependence of σ for an applied field of 50 mT. The inset shows the temperature dependence of the internal magnetic field at the muon site with the expected diamagnetic shift below T_c. The solid line is a guide to the eye.

The superconducting contribution to σ is obtained by subtracting the nuclear moment contribution (measured above T_c) as ${\sigma_{sc}}^2 = \sigma^2 - {\sigma_{nm}}^2$. In an isotropic type-II superconductor with a hexagonal Abrikosov vortex lattice described by Ginzburg-Landau theory, the magnetic penetration depth λ is related to σ_{sc} by the equation [17]:

$$\sigma_{sc}(b)\ [\mu s^{-1}] = 4.854 \times 10^4 (1-b) \times [1 + 1.21(1-\sqrt{b})^3]\lambda^{-2} \quad [nm^{-2}]. \tag{6}$$

Here $b = \langle B\rangle/B_{c2}$ is a reduced magnetic field. In calculating λ, we have used the temperature dependence of $B_{c2} = \mu_0 H_{c2}$ as shown in Fig. 2(c).

Figure 5(b) shows the temperature dependence of λ^{-2} (which is proportional to the superfluid density ρ_s). Below 1 K, $\lambda^{-2}(T)$ appears to flatten as is the case for fully gapped superconductors. This indicates that there are no nodes in the energy gap of $Sr_3Ir_4Sn_{13}$. The solid lines in Fig. 5(b) represent fits to the data with a single- and a two-gap BCS s-wave model

TABLE I. Parameters of the fits to the $\lambda^{-2}(T)$ data of $Sr_3Ir_4Sn_{13}$ using different gap models. The errors given are the statistical error from the fit.

Model	Gap value $\Delta(0)$ (meV)	Gap ratio $\Delta(0)/k_BT_c$	χ^2_{reduced}
s wave	0.82(2)	2.1(1)	1.36
s+s wave	0.91(4), 0.14(7) with $\omega = 0.92(3)$	2.4(1), 0.4(2)	1.03

using the following functional form [20,21]:

$$\frac{\lambda^{-2}(T)}{\lambda^{-2}(0)} = \omega\frac{\lambda^{-2}(T,\Delta_1(0))}{\lambda^{-2}(0,\Delta_1(0))} + (1-\omega)\frac{\lambda^{-2}(T,\Delta_2(0))}{\lambda^{-2}(0,\Delta_2(0))}, \quad (7)$$

where $\lambda(0)$ is the value of the penetration depth at $T = 0$ K, $\Delta_i(0)$ is the value of the ith ($i = 1$ or 2) superconducting gap at $T = 0$ K, and ω is the weighting factor of the large gap.

Each component of Eq. (7) can be expressed within the local London approximation ($\lambda \gg \xi$) [22,23] as

$$\frac{\lambda^{-2}(T,\Delta_i(0))}{\lambda^{-2}(0,\Delta_i(0))} = 1 + 2\int_{\Delta_i(0)}^{\infty}\left(\frac{\partial f}{\partial E}\right)\frac{EdE}{\sqrt{E^2-\Delta_i(T)^2}}, \quad (8)$$

where $f = [1+\exp(E/k_BT)]^{-1}$ is the Fermi function, and $\Delta_i(T) = \Delta_i(0)\delta(T/T_c)$. Approximating the temperature dependence of the gap [20,21] by $\Delta(T) = \Delta(0)\tanh\{1.82[1.018(T_c/T-1)]^{0.51}\}$, the fit yields $T_c = 4.56(7)$ K, $\lambda(0) = 291(3)$ nm, and $\Delta(0) = 0.82(2)$ meV for the s-wave model. The gap to T_c ratio $\Delta(0)/k_BT_c = 2.1(1)$ is higher than the BCS value of 1.76, suggesting that $Sr_3Ir_4Sn_{13}$ is a strong-coupling superconductor. Using H_{c2} as determined from resistivity measurements [15] in Eq. (6) does not change these values appreciably: $\lambda(0) = 311(3)$ nm, $\Delta(0) = 0.79(2)$ meV, and $\Delta(0)/k_BT_c = 2.0(1)$. This is due to the fact that the applied field we used was only 50 mT and that the correction in Eq. (6) is small for the relevant temperature range.

The fit to the $\lambda^{-2}(T)$ data can be improved by using a two-gap $s+s$-wave model. Table I summarizes the corresponding fitted parameters. The two-gap s+s-wave model gives a lower χ^2_{reduced} value than a single gap model indicating that $Sr_3Ir_4Sn_{13}$ might be a multigap superconductor. This is consistent with calculations showing multiple bands crossing the Fermi surface [1].

Using $\mu_0H_{c2}(0) = 1.44(2)$ T and its relation with the coherence length ξ, ($\mu_0H_{c2} = \frac{\phi_0}{2\pi\xi^2}$), we calculate $\xi = 15.1(2)$ nm at 0 K. This gives a $\kappa = \frac{\lambda}{\xi} \simeq 19$.

By combining the value of ξ and our measured value of λ, we can calculate the value of H_{c1} using the expression [22]:

$$\mu_0H_{c1} = \frac{\phi_0}{4\pi\lambda^2}\left(\ln\frac{\lambda}{\xi} + 0.5\right). \quad (9)$$

We estimate $\mu_0H_{c1}(0) = 6(1)$ mT, which is in reasonable agreement with the μ_0H_{c1} value of 8.5(1) mT, extracted from the magnetization measurements. Our values of $\Delta(0)$ and gap-to-T_c ratio obtained by microscopic measurements are in good agreement with those obtained from specific heat measurements, [5] whereas $\xi(0)$ is slightly larger [and $\lambda(0)$ smaller] than in Ref. [5], indicating a cleaner material.

In conclusion, magnetization and μSR measurements have been performed on superconducting $Sr_3Ir_4Sn_{13}$. From the magnetization measurements we determine the temperature dependence of the lower and upper critical fields. The ZF-μSR results provide no evidence for any electronic magnetic moments or magnetic order in $Sr_3Ir_4Sn_{13}$, but show that below T^* there is a small increase in the muon spin relaxation rate consistent with a structural and/or CDW scenario accompanied by a lattice distortion.

TF-μSR results show that the superfluid density ρ_s, which is proportional to λ^{-2}, has a temperature dependence that is consistent with a fully gapped superconducting state, with $\rho_s(T)$ well described within the single s-wave gap scenario with $\Delta(0) = 0.82(2)$ meV and penetration depth $\lambda(0) = 291(3)$ nm. The value of the gap to T_c ratio, 2.1(1), is higher than the BCS value of 1.76 and indicates that $Sr_3Ir_4Sn_{13}$ is a strong-coupling superconductor. Recently [24], we found a similar gap to T_c ratio of 2.41(8) in the isoelectronic compound $Ca_3Ir_4Sn_{13}$ at variance with the unusual ratio of ~5 reported in Ref. [7]. It is worth mentioning that even though we can make a reasonable fit to the data with a single-gap model, a two-gap model (showing a lower χ^2_{reduced} value) is also consistent with the temperature dependence of the superfluid density. Multigap superconductivity in $Sr_3Ir_4Sn_{13}$ may arise from the multiband structure of this material. However, the uncertainty in both the values [$\Delta(0) = 0.14(7)$ meV] and weight [8(3)%] of the small gap mean that more detailed studies are required before a definite statement can be made on this matter. The results presented here will provide a reference point for studies under pressure to detect changes of the superconducting and magnetic properties in this and related materials. The prospect of suppressing the CDW gap at T^* and increasing T_c under hydrostatic pressure provides a good motivation for μSR and other studies under pressure which could be used to better understand the interplay between superconductivity and charge ordering in the ternary intermetallic stannides.

The μSR experiments were performed at the Swiss Muon Source (SμS), Paul Scherrer Institute (PSI, Switzerland). Work at Brookhaven is supported by the US DOE under Contract No. DE-AC02-98CH10886.

[1] L. E. Klintberg, S. K. Goh, P. L. Alireza, P. J. Saines, D. A. Tompsett, P. W. Logg, J. Yang, B. Chen, K. Yoshimura, and F. M. Grosche, Phys. Rev. Lett. **109**, 237008 (2012).

[2] G. P. Espinosa, Mater. Res. Bull. **15**, 791 (1980).

[3] J. Yang, B. Chen, C. Michioka, and K. Yoshimura, J. Phys. Soc. Jpn. **79**, 113705 (2010).

[4] K. Wang and C. Petrovic, Phys. Rev. B **86**, 024522 (2012).
[5] N. Kase, H. Hayamizu, and J. Akimitsu, Phys. Rev. B **83**, 184509 (2011).
[6] S. Y. Zhou, H. Zhang, X. C. Hong, B. Y. Pan, X. Qiu, W. N. Dong, X. L. Li, and S. Y. Li, Phys. Rev. B **86**, 064504 (2012).
[7] S. Gerber, J. L. Gavilano, M. Medarde, V. Pomjakushin, C. Baines, E. Pomjakushina, K. Conder, and M. Kenzelmann, Phys. Rev. B **88**, 104505 (2013).
[8] H. Hayamizu, N. Kase, and J. Akimitsu, J. Phys. Soc. Jpn. **80**, SA114 (2011).
[9] A. Aharoni, J. Appl. Phys. **83**, 3432 (1998).
[10] A. Suter and B. M. Wojek, Physics Procedia **30**, 69 (2012).
[11] A. Umezawa, G. W. Crabtree, J. Z. Liu, T. J. Moran, S. K. Malik, L. H. Nunez, W. L. Kwok, and C. H. Sowers, Phys. Rev. B **38**, 2843 (1988).
[12] T. H. Johansen, M. R. Koblischka, H. Bratsberg, and P. O. Hetland, Phys. Rev. B **56**, 11273 (1997).
[13] N. R. Werthamer, E. Helfand, and P. C. Hohenberg, Phys. Rev. **147**, 295 (1966).
[14] E. Helfand and N. R. Werthamer, Phys. Rev. **147**, 288 (1966).
[15] Magneto-resistance measurements give a higher $\mu_0 H_{c2}(0) = 3.7$ T. However, such a determination may be influenced by impurity phases.
[16] R. Kubo, Hyperfine Interact. **8**, 731 (1981).
[17] E. H. Brandt, Phys. Rev. B **68**, 054506 (2003).
[18] M. Weber, A. Amato, F. N. Gygax, A. Schenck, H. Maletta, V. N. Duginov, V. G. Grebinnik, A. B. Lazarev, V. G. Olshevsky, V. Yu. Pomjakushin, S. N. Shilov, V. A. Zhukov, B. F. Kirillov, A. V. Pirogov, A. N. Ponomarev, and V. G. Storchak, S. Kapusta, and J. Bock, Phys. Rev. B **48**, 13022 (1993).
[19] A. Maisuradze, R. Khasanov, A. Shengelaya, and H. Keller, J. Phys.: Condens. Matter **21**, 075701 (2009).
[20] A. Carrington and F. Manzano, Physica C **385**, 205 (2003).
[21] H. Padamsee, J. E. Neighbor, and C. A. Shiffman, J. Low Temp. Phys. **12**, 387 (1973).
[22] M. Tinkham, *Introduction to Superconductivity* (McGraw-Hill, New York, 1975).
[23] R. Prozorov and R. W. Giannetta, Supercond. Sci. Technol. **19**, R41 (2006).
[24] P. K. Biswas, A. Amato, Kefeng Wang, C. Petrovic, R. Khasanov, H. Luetkens, and E. Morenzoni, Proceedings of the 13th International Conference on Muon Spin Rotation/Relaxation and Resonance, Grindelwald, J. Phys.: Conf. Ser. (2014) (to be published).